PAPER • OPEN ACCESS

Simulation of Aldehyde Emissions from an Ethanol Fueled Spark Ignition Engine and Comparison with FTIR Measurements

To cite this article: Paola Helena Barros Zaránte and Jose Ricardo Sodre 2016 *J. Phys.: Conf. Ser.* **745** 032023

View the article online for updates and enhancements.

Related content

IOP ebooks™

Bringing you innovative digital publishing with leading voices to create your essential collection of books in STEM research.

Start exploring the collection - download the first chapter of every title for free.

Simulation of Aldehyde Emissions from an Ethanol Fueled Spark Ignition Engine and Comparison with FTIR Measurements

Paola Helena Barros Zarante

Universidad del Atlántico, Department of Mechanical Engineering
km 7 - Antigua vía Puerto Colombia - Barranquilla – Colombia

José Ricardo Sodré

Pontifical Catholic University of Minas Gerais, Department of Mechanical
Engineering, Belo Horizonte, MG, Brazil

E-mail: ricardo@pucminas.br

Abstract. This paper presents a mathematical model that calculates aldehyde emissions in the exhaust of a spark ignition engine fueled with ethanol. The numerical model for aldehyde emissions was developed using FORTRAN software, with the input data obtained from a dedicated engine cycle simulation software, AVL BOOST. The model calculates formaldehyde and acetaldehyde emissions, formed from the partial oxidation of methane, ethane and unburned ethanol. The calculated values were compared with experimental data obtained by Fourier Transform Infrared Spectroscopy (FTIR). The experiments were performed with a mid-size sedan powered by a 1.4-liter spark ignition engine on a chassis dynamometer. In general, the results demonstrate that the concentrations of aldehydes and the source elements increased with engine speed and exhaust gas temperature. A reasonable agreement between simulated and measured values was achieved.

1. Introduction

Ethanol is an attractive alternative fuel for spark ignition engines, from the viewpoint of regulated emissions. The addition of ethanol to gasoline improves fuel economy and reduces emissions of CO, HC and NO_X from spark ignition engines [1]. However, the incomplete combustion of ethyl alcohol in the engine exhaust produces high concentrations of aldehydes (RCHO). Aldehydes are highly reactive organic compounds that participate in complex chemical reactions in the atmosphere. Only the aldehydes encountered in the gaseous state are considered pollutants in internal combustion engines: formaldehyde (CH_2O) and acetaldehyde (C_2H_4O). The emissions of aldehydes are higher for ethanol fuel due to the presence of the hydroxyl functional group (OH), absent in gasoline [2].

The ethanol–gasoline blend fuel could improve emissions other species. Dynamometer tests conducted by [3] on a 1.4-liter, flexible fuel spark ignition engine showed that hydrous ethanol addition to gasoline with 25% v/v of anhydrous ethanol reduced CO and total HC, but increased carbon dioxide (CO_2), aldehydes and unburned ethanol emissions. The concentrations were measured by a Fourier

transform infrared (FTIR) analyzer.

The results obtained by [4] on a spark ignition engine fueled with hydrous ethanol with up to 40% water content show that increasing load decreased HC, formaldehyde and acetaldehyde emissions. In [5] different percentages of alcohol blend and fumigation were summarized to get information about the effect of alcohol on regulated and unregulated emissions of IC engines. For unregulated emissions, it was seen an increase of unburned ethanol and methanol and total carbonyls in all tests. And, an increase of formaldehyde and acetaldehyde which are the predominant carbonyls in the exhaust for vehicles was recorded in most and major experiments, respectively for both modes. [6] show that benzaldehyde, acetaldehyde, formaldehyde and volatile organic compounds (VOCs) are the dominant emission products from bioethanol, similarly to ethanol–gasoline blends. From tests in a single cylinder spray guided direct-injection spark-ignition (DISI) engine, [7] observed much lower formaldehyde and acetaldehyde emissions for 2-Methylfuran (MF) and 2,5-dimethylfuran (DMF), compared to gasoline, ethanol and methanol. Formaldehyde emission from ethanol (155.7 ppm) was slightly lower than that from gasoline (179.4 ppm). However, acetaldehyde emission from ethanol (303.1 ppm) was much higher than that of gasoline (53.9 ppm).

The study developed by [8] experiments were carried out in this spark ignition (SI) engine, which was fueled by gasohols (E5, E15, M5 and M15) for characterizing regulated and unregulated emissions. A Fourier transform infrared (FTIR) emission analyzer was used for unregulated emission measurements. For higher gasohol blends (E15), ethyl alcohol, formaldehyde, propane and *iso*-butylene emissions were present in relatively higher concentrations in the exhaust. M15 emitted higher concentrations of methanol, formaldehyde, propane, *n*-pentane, and toluene compared to other test fuels. Acetaldehyde was emitted by gasoline–ethanol blends however it was not detected in the emissions from gasoline and gasoline–methanol blends.

In order to describe the chemical reactions occurring during ethanol combustion, detailed kinetic models were developed by authors such as [9], [10] and [11]. These models simulate the chemical reactions within reactors used for combustion studies. However, they exhibit great chemical complexity, requiring several hundreds of reactions to reach the results. A kinetic model, previously elaborated by [12], has been improved by building a complete sub-mechanism taking into account the formation and consumption of species involved in formaldehyde formation. The improved mechanism contains 107 chemical species and 568 reactions in order to simulate formaldehyde formation accurately. The reliability of the kinetic model has been tested in ethanol flames.

Viggiano and Maci [13] analyzed the emissions from an ethanol fueled homogeneous charge compression ignition (HCCI) engine through a multidimensional numerical solver coupled to a kinetic reaction mechanism. The model is made up of 235 reaction steps among 43 chemical species for ethanol oxidation, and a NO_X kinetic reaction mechanism made up of 53 reaction steps among 14 chemical species. The combustion model accounts for the influence of turbulent time scale on the kinetic time scale. Several dynamic adaptive chemistry (DAC) computations have been performed by [14] using two kinetic reaction mechanisms of ethanol combustion in HCCI engines with different levels of detail that include 57 species and 135 species, respectively. The simulations show that very accurate results of pressure and heat release rate profiles and CO, CO_2 and unburned HC emissions are obtained for both uniform fuel distribution and direct injection of liquid fuel in the combustion chamber. For the single-zone computations, the use of DAC provides a speed-up the 135-species full mechanism more than 9 times.

Vuilleumier et al. [15] examines intermediate temperature heat release (ITHR) in HCCI engines using blends of ethanol and n-heptane. The simulation results were used to identify the dominant reaction pathways contributing to ITHR, as well as to verify the chemical basis behind the quantification of the amount of ITHR in the experimental analysis. The detailed chemical kinetic mechanism for n-heptane was developed in a hierarchical manner, and therefore includes detailed chemistry for ethanol combustion. The ethanol sub-mechanism is largely based on the original work of [9]. A previous work [16] has focused on building sub-models to predict the gas dynamics, combustion and knock occurrence in alcohol engines. The building blocks are implemented in a quasi-dimensional engine simulation code, which is subsequently validated against measurements on two engines for various conditions.

Vourliotakis et al. [17] utilized a single, in-house developed, detailed chemical kinetic mechanism to model and analyze five stoichiometric or near stoichiometric low-pressure laminar premixed flames of C1–C2 oxygenated fuels. Flames of the two smallest aldehydes (formaldehyde and acetaldehyde) and

the two smallest alcohols (methanol and ethanol) are considered. The mechanism is shown to satisfactorily reproduce fuel decay as well as major and intermediate species profiles. Reaction path analysis is extensively utilized in order to scrutinize the controlling elementary steps.

This paper describes a model of formaldehyde and acetaldehyde formation in the engine exhaust from methane, ethane and unburned ethanol oxidation, formed as intermediate products of ethanol combustion. The chemical kinetic model developed in [18] presents aldehyde formation in internal combustion engines fueled by gasoline or ethanol and it was taken as a basis for this work. The results from the simulation are compared with experimental data from laboratory tests in a production vehicle, with exhaust aldehydes being measured by Fourier Transform Infrared (FTIR).

2. Methodology

The description of the methodology here applied is divided into the aldehyde formation model, model simulation and the experiments performed to compare with the model results.

2.1. Aldehyde Formation

The methodology used to simulate formaldehyde and acetaldehyde formation is based on the theory of chemical reaction kinetics applied to aldehyde formation from in-cylinder ethanol combustion. The aldehyde formation reactions start in the cylinder and propagate through the exhaust pipe. The differential equations of the chemical reactions in the cylinder and the exhaust pipe are time-integrated, obtaining algebraic expressions for the concentrations of formaldehyde, acetaldehyde, methane and ethane.

The aldehyde simulation model considers that exhaust acetaldehyde (CH_3CHO) is mainly formed in the intermediate phase of the post-flame oxidation of unburned ethanol (CH_3CH_2OH) in the combustion chamber and in the exhaust pipe, according to:

$$CH_3CH_2OH + [O] \rightarrow CH_3CHO + H_2O \tag{1}$$
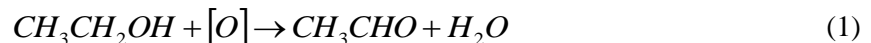
Formaldehyde and acetaldehyde are also formed from the post-flame oxidation process of methane (CH_4) and ethane (C_2H_6), respectively. These components are generated when the decomposition process of the unburned fuel in the exhaust gas is stopped at an intermediate stage of the chemical reaction. The interruption is mainly due to reduction of temperature and oxygen concentration. The first product of methane oxidation is methanol, which is immediately oxidized to formaldehyde in the presence of oxygen remaining in the general reaction:

$$CH_4 + O_2 \rightarrow CH_2O + H_2O \tag{2}$$
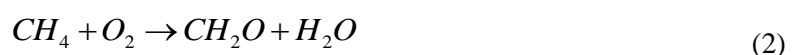
The production of acetaldehyde from ethane oxidation is given by:

$$C_2H_6 + O_2 \rightarrow C_2H_4O + H_2O \tag{3}$$

The aldehydes formed in the intermediate stages of the combustion process are immediately consumed by the flame front due to the high temperature attained in the combustion chamber. In order to calculate the exhaust aldehyde concentration, the oxidation reactions are considered separately, being the final concentration given by the sum of the parts produced in each reaction.

Aldehyde formation is calculated from the combustion chamber to the sampling point in the exhaust pipe. While the concentration of unburned ethanol is given by the BOOST software, the concentrations of methane, ethane, formaldehyde and acetaldehyde are calculated by the aldehyde emission model from the reaction equations presented in [9] and [18]. The calculation is performed from the moment the exhaust valve opens until the end of the exhaust process.

The exposure of methane to oxygen causes an oxidation process that forms formaldehyde and water molecules. The methanol formed in the intermediate phase of methane oxidation to formaldehyde is oxidized instantaneously, as shown by Eqs. (4) and (5) [18]:

$$CH_4 + \tfrac{1}{2}O_2 \rightarrow CH_3OH \tag{4}$$

$$CH_3OH + \tfrac{1}{2}O_2 \rightarrow HCHO + H_2O \tag{5}$$
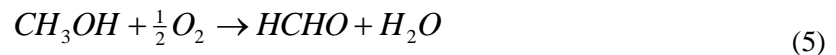
Therefore, the formation rate of formaldehyde (*HCHO*) from methane (*CH₄*) oxidation takes the form [18]:

$$\frac{d[HCHO]}{dt} = A \cdot T^n \cdot \exp\left(\frac{-E_A}{R \cdot T}\right) \cdot \frac{7200}{(R \cdot T)^{1/2}} \cdot \exp\left(\frac{-69.090}{T}\right) \cdot [O_2]^{1/2} \cdot [CH_4] \tag{6}$$

Where A is the pre-exponential factor of Arrhenius ($6,46 \times 10^{14}$ *cm³/gmol.s*) [10], T the temperature (K), n is the exponent of the temperature, E_A the activation energy (179,9 *kJ/gmol*) [10] and R the universal gas constant ($8,31434 \times 10^{-3}$ *kJ/gmol.K*) [18].

Acetaldehyde formation from ethane oxidation is given by [18]:

$$C_2H_6 + \tfrac{1}{2}O_2 \rightarrow C_2H_5OH \tag{7}$$

$$C_2H_5OH + \tfrac{1}{2}O_2 \rightarrow C_2H_4O + H_2O \tag{8}$$
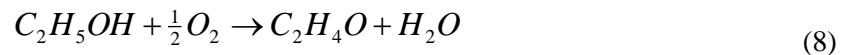
Following similar procedure to methane oxidation, the mathematical model that represents the rate of formation of acetaldehyde (C₂H₄O) from ethane (C₂H₆) oxidation of is so given [18]:

$$\frac{d[C_2H_4O]}{dt} = A \cdot T^n \cdot \exp\left(\frac{-E_A}{R \cdot T}\right) \cdot \frac{7200}{(R \cdot T)^{1/2}} \cdot \exp\left(\frac{-69.090}{T}\right) \cdot [O_2]^{1/2} \cdot [C_2H_6] \tag{9}$$

Where constants A and E_A assume the values of $3,98 \times 10^{13}$ *cm³/gmol.s* and 213,0 *kJ/gmol*, respectively [18]. The unit of measure for acetaldehyde formation rate given by Eq. (8) is *gmol/cm³.s*.

Ethanol oxidation to acetaldehyde, which begins in the region after the flame front in the combustion chamber and propagates along the exhaust pipe, is written as [18]:

$$C_2H_5OH + \tfrac{1}{2}O_2 \rightarrow C_2H_4O + H_2O \tag{10}$$
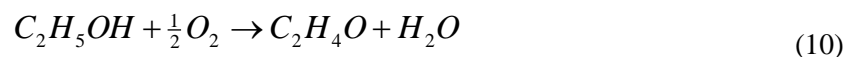
Using a similar mechanism as that described for methane and ethane oxidation, ethanol oxidation is initiated by developing the rate of formation of the reaction products represented by Eq. (10). Thus, the rate of formation of acetaldehyde (C₂H₄O) from ethanol oxidation is given by [18]:

$$\frac{d[C_2H_4O]}{dt} = A \cdot T^n \cdot \exp\left(\frac{-E_A}{R \cdot T}\right) \cdot \frac{7200}{(R \cdot T)^{1/2}} \cdot \exp\left(\frac{-69.090}{T}\right) \cdot [O_2]^{1/2} \cdot [C_2H_5OH] \tag{11}$$

Where constants A and E_A assume the values of $1,12 \times 10^{13}$ *cm³/gmol.s* and 127,3 *kJ/gmol*, respectively [18]. The unit of measure for acetaldehyde formation rate given by Eq. (11) is *gmol/cm³.s*.

2.2. Numerical Simulation

The dedicated software AVL BOOST was used to simulate the cycle of an ethanol-fueled, four-stroke spark ignition engine, with main interest on combustion and exhaust emissions. The flow in the pipes is treated by the software as one-dimensional. This means that the pressures, temperatures and flow velocities obtained from the solution of the gas dynamic equations represent mean values over the cross-section of the pipes [19]. The input data for the simulation correspond to the engine used in the experiments performed to compare with the model.

The AVL BOOST software is not able to calculate aldehyde emissions. The calculated cylinder

temperature and pressure diagrams throughout the cycle and the exhaust concentrations of oxygen and unburned ethanol are used as input data for the aldehyde emissions model here developed in FORTRAN code. The routine developed in the FORTRAN software works with the chemical reaction equations to calculate the concentrations of aldehydes and their producers in the cylinder and exhaust pipe. The simulation was performed varying the engine crankshaft speed from 2000 rpm to 5000 rpm.

2.3. Experiments
The model results were compared with experimental data obtained from a 4 cylinder, 1.4 liters, 10.35:1 compression ratio, 60 kW rated power, 121 N.m rated torque, FIAT FIRE 1.4 Flex spark ignition engine, operated in a bench test dynamometer, fueled with hydrous ethanol (6.8% wt./wt. of water). K-type thermocouples, with uncertainty of reading of ± 2°C, were installed in the engine to measure the intake air temperature and the exhaust gas temperature. The exhaust gas sample was taken from the exhaust pipe, close to the exhaust port, and driven through a heated sampling line, to avoid heavy component condensation, into a FTIR analyzer. The measurements were made with the engine operating at steady state condition, wide open throttle, air/fuel equivalence ratio 0.96, variable load and crankshaft speeds of 2000, 3000, and 4000 rpm, with corresponding ignition timings of 25.7°BTDC, 29.3°BTDC and 27.9°BTDC, respectively. The results shown in the following section are the average of three tests performed at each engine operating condition.

3. Results
The results from the simulation are compared with experimental values measured by Fourier Transform Infrared spectroscopy (FTIR). The concentrations of formaldehyde, acetaldehyde and their main producers – methane, ethane and unburned ethanol – were measured. Acetaldehyde corresponds to the sum of the parts formed from the post-flame oxidation of unburned ethanol and ethane. All substances present a trend of increased concentration with increasing engine speed, as can be seen in Figures 1 to 5. Model and experiments generally show qualitative agreement, while the proximity of the quantitative values depends on the engine operating condition.

The general trends obtained for formaldehyde and acetaldehyde, shown in Figures 1 and 2, are in agreement with [20] and [21] and [22], who also found increased aldehyde concentration with engine speed. It is observed that the concentrations of measured and simulated acetaldehyde are larger than those of formaldehyde, as found in [21], using ethanol as fuel, and in [22], [23], [24] and [25], for ethanol blends. The acetaldehyde concentration levels found in [20] and [21] are close to those found in the present work (Figure 2).

The increase of formaldehyde (Figure 1) and acetaldehyde (Figure 2) concentrations with engine speed is due to the increase of exhaust gas temperature with engine speed [18], together with the increase of the concentrations of methane (Figure 3), ethane (Figure 4) and unburned ethanol (Figure 5). The increase of exhaust gas temperature with engine speed is due to the shorter time for the engine cycle to be complete, making combustion finish later in the cycle. Thus, when the exhaust valve opens it finds the burned gas in the cylinder at a higher temperature. The gas temperature and the concentrations of methane, ethane and unburned ethanol are the main factors to affect aldehyde formation in the model.

The trend obtained for methane measured by FTIR analysis (Figure 3) is not the same as that found for the measured formaldehyde (Figure 1), of which methane is the main producer. However, the simulated trends of methane and formaldehyde are similar (Figures 1 and 3). The simulated values of formaldehyde underestimates the measured values in the whole range investigated, showing larger discrepancies at 2000 rpm and 3000 rpm (Fig. 1). That is a direct consequence of the simulated values of methane also underestimating the measured values in the whole speed range (Fig. 3), once formaldehyde is formed during methane oxidation process. Both reaction rates of methane formation from ethanol oxidation and formaldehyde formation from methane oxidation requires further investigation. The simulated and measured values of ethane have a close resemblance (Figure 4). The exhaust methane concentration is always higher than ethane concentration at any engine speed (Figures 3 and 4).

From Figure 5 it is observed that the simulated ethanol concentrations are very high in comparison with the measured values obtained by FTIR. That is because of the intense oxidation of unburned ethanol that continues from the sampling point in the exhaust through the sampling line until reaching the analyzer, thus reducing unburned ethanol concentration. The simulation only takes into consideration variations on ethanol concentration from the combustion chamber until the sampling point. The trend

shown by exhaust unburned ethanol is clearly the same as that of acetaldehyde (Figure 2). The studies of [23] and [26] confirm these results: an increase in the concentration of unburned ethanol is associated with the increase of acetaldehyde concentration. With the increase of engine speed, the rate of fuel mass injected into the cylinder is increased, thus increasing the amount of unburned fuel remaining after combustion.
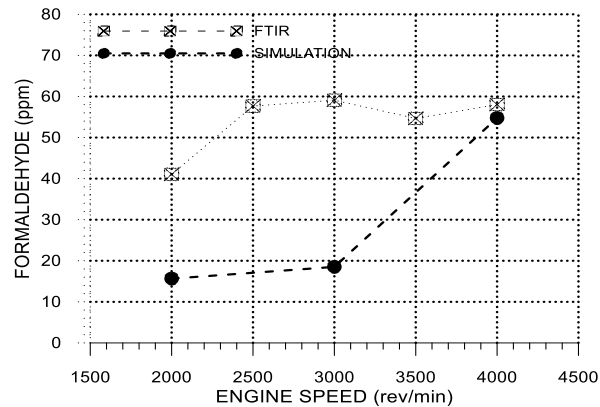

Figure 1. Simulated and measured (FTIR) concentrations of exhaust formaldehyde.
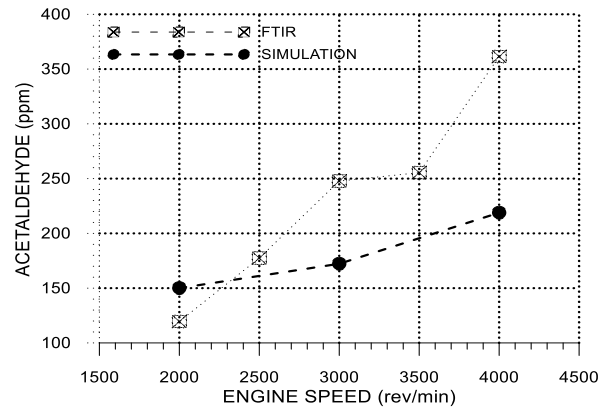
Figure 2. Simulated and measured (FTIR) concentrations of exhaust acetaldehyde.
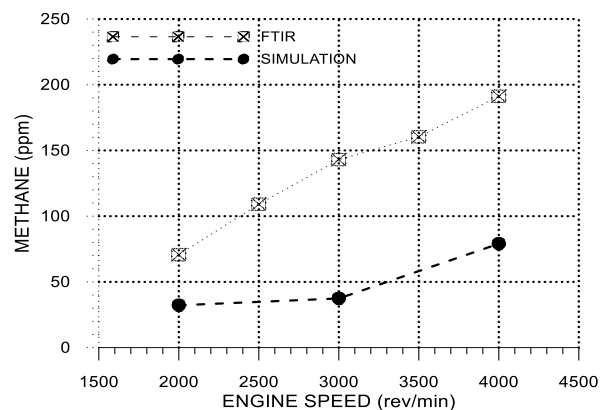

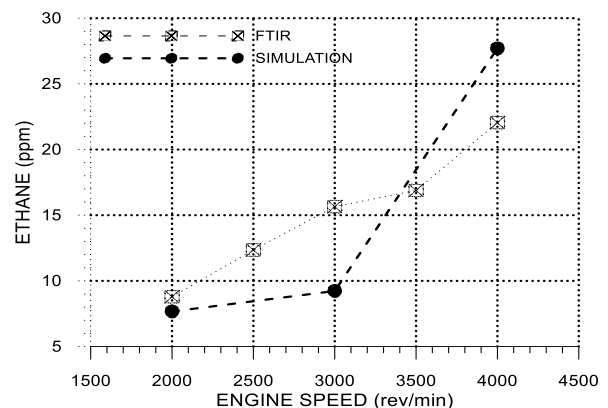**Figure 3.** Simulated and measured (FTIR) concentrations of exhaust methane.

Figure 4. Simulated and measured (FTIR) concentrations of exhaust ethane.
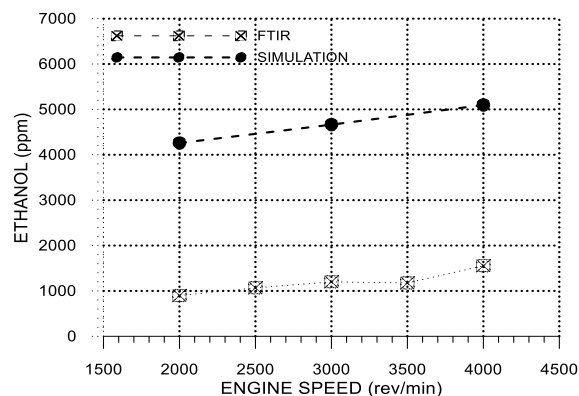

Figure 5. Simulated and measured (FTIR) concentrations of exhaust unburned ethanol.

In order to increase the engine speed a higher amount of fuel is injected in the engine and, at the same time, combustion becomes more inefficient because of the shorter period it is allowed to be completed

and the lesser amount of air admitted by cycle. That is the reason why the concentration of exhaust ethanol is increased with engine speed (Figure 5). As intermediate products of the post-flame oxidation of higher amounts of unburned ethanol in the presence of higher exhaust gas temperature, higher amounts of methane (Figure 3) and ethane (Figure 4) are also produced with increasing engine speed.

4. Conclusions

A new model for exhaust aldehyde formation in spark ignition engines has been presented and comparisons were made against experimental data. The simulated values of exhaust formaldehyde, acetaldehyde and their main producers – methane, ethane and unburned ethanol – show good qualitative agreement and reasonable quantitative agreement with the measured values by FTIR analysis. The highest discrepancies found between the simulated results and the measured data was for exhaust unburned ethanol. The simulation model was proved to be a useful tool to estimate exhaust formaldehyde and acetaldehyde from an engine operating with ethanol as fuel. The FTIR analysis was able to measure exhaust aldehyde concentration, even the low amounts presented by formaldehyde. Both the model and the experiments show increased concentrations of exhaust formaldehyde, acetaldehyde, methane, ethane and unburned ethanol with increasing engine speed. These results were attributed to, at higher engine speeds, the lower period allowed to complete the combustion process, making it more inefficient and increasing the exhaust gas temperature, which is a key parameter for aldehyde formation.

5. Acknowledgements

References

[1]   Keating E 1993 *Applied Combustion* (New York: Marcel Dekker).
[2]   Basshuysen R and Schäfer F 2004 *Internal Combustion Engine Handbook: Basics, Components, Systems, and Perspectives*. (Warrendale: SAE International)
[3]   Melo T, Machado G, Belchior C, Colaço M, Barros J, Oliveira E and Oliveira D 2012 *Fuel* **97** 796.
[4]   Munsin R, Laoonual Y, Jugjai S and Imai Y 2013 *Fuel* **106** 586.
[5]   Ghadiokolaei M 2016 *Renewable and Sustainable Energy Reviews* **57** 1440.
[6]   Manzetti S and Andersen O 2014 *Fuel* **140** 293.
[7]   Wang Ch, Xu H, Daniel R, Ghafourian A, Herreros J, Shuai Sh and Ma X 2013 *Fuel* **103** 200.
[8]   Agarwal A, Shukla P, Gupta J, Patel C, Prasad R, Sharma N 2015 *Applied Energy* **154** 732.
[9]   Marinov N 1999 *Int. J. Chem. Kinetics* **31** 183.
[10] Li J, Kazakov A, Chaos M. and Dryer F 2007 *Proc. 5th US Combustion Meeting* (San Diego: Western States Section of the Combustion Institute).
[11] Frassoldati A, Cuoci A, Faravelli T, Niemann U, Ranzi E, Seiser R and Seshadri K 2010 *Comb. Flame* **157** 2.
[12] Dias V, Duynslaegher C, Contino F, Vandooren J and Jeanmart H 2012 *Comb. Flame* **159** 1814.
[13] Viggiano A and Magi V 2012 *Appl. Energy* **93** 277.
[14] Viggiano A and Magi V 2014 *Appl. Energy* **113** 848.
[15] Vuilleumier D, Korzarac D, Mehl M, Saxena S, Pitz W, Dibble R, Chen J-Y and Sarathy S 2014 *Combustion and Flame* **161** 680.
[16] Vancoillie J, Sileghem L and Verhelst S 2014 *Appl. Energy* 132 412.
[17] Vourliotakis G, Skevis G and Founti M 2015 *Proc. Comb. Inst*. **35** 437.
[18] Costa T Zarante P and Sodré J In: Sens M, Baar R, editors 2013 *Engine processes* (Berlin: Expert Verlag).
[19] AVL BOOST V2010 2010 *Users Guide* (Austria: AVL List GmbH).
[20] Amaral R and Sodré J 2001 *Proc. Inter. Spring Fuels & Lubricant Meeting* SAE Technical Paper 2001-01-1998 (USA: Society of Automotive Engineers).
[21] Amaral R and Sodré J 2002 *Comb. Sci. Technol.* **174** 153.
[22] Pang X Um Y Yuan J and He H 2008 *Atmos. Environ.* **42** 1349.

[23] He B-Q Shuai S-J Wang J-X and He H 2003 *Atmos. Environ*. **37** 4965.
[24] Song C Zhao Z Liv G Song J Liu L and Zhao R 2010 *Chemosphere* **79** 1033.
[25] Magnusson S and Nilsson C 2011 *Fuel* **90** 1145.
[26] Cheung C Di Y and Huang Z 2008 *Atmos. Environ.* **42** 8843.